

CONVEX OPTIMIZATION FOR FAST IMAGE DEHAZING

Jiaxi He*

Cishen Zhang*

Ran Yang*†

Kai Zhu*†

*School of Software and Electrical Engineering

Swinburne University of Technology, Victoria 3122, Australia

†School of Information and Mobile Engineering, Sun Yat-Sen University, Guangzhou 510275, China

† NICTA, West Melbourne, Victoria 3003, Australia

ABSTRACT

This paper presents a new convex optimization method for the image dehazing problem. It is based on reformulation of the hazed image model to solve the bilinearly coupled hazed image and light transmission distribution term as a single optimization variable. This resolves the nonconvex difficulty of the original problem and is sufficient for straightforward reconstruction of the haze free image. The Haar wavelet transform is further applied to derive a subband hazed image model for the convex optimization, which leads to great reduction of the computational workload.

Index Terms— Image Dehazing, Convex Optimization, Wavelet Transform

1. INTRODUCTION

Haze occurs when dust and smoke particles accumulate in atmosphere, which causes light scattering through the haze particles and consequently degrades the visibility and contrast in images and videos. The image dehazing problem is to apply post processing of hazed images to remove the haze effects and recover the original image scene, which has been an active area in image processing in recent years. The optical image model shows that the image dehazing is a nonconvex problem because of the bilinearly coupled haze free image and atmosphere light transmission distribution.

The general idea of image dehazing is to reconstruct the haze free images by regulating and sharpening the image contrast and details. Many existing image dehazing algorithms require additional information or strong prior of images such as the image orientation [1, 2], multiple images [3, 4], 3-dimensional geometric information [5, 6], near inferred technique [7, 8], or dark channel prior [9–13]. A number of algorithms use the Markov random field to model the haze scene [14–20], which is based on probability analysis of the spatial and contextual dependencies of physical phenomena.

This paper presents a new convex optimization method to solve the image dehazing problem. It is observed that the bilinearly coupled haze free image and atmosphere light trans-

mission distribution, as a whole single term, is linear in the hazed image model. Based on this observation, a convex optimization problem is formulated to solve the bilinearly coupled term and the atmosphere light transmission distribution as linear optimization variables. This resolves the nonconvex difficulty of the original problem. Its solution can be effectively solved by standard regularized convex optimization and is sufficient for straightforward reconstruction of the haze free image. To further improve the computational efficiency, the Haar wavelet transform is applied to derive a subband hazed image model with reduced dimension. Using an assumption on the low pass and piecewise smoothness of the atmosphere light transmission distribution, it is shown that to solve the dehazing problem of the subband model with the reduced dimension is sufficient for the solution of the original dehazing problem. This results in significant reduction of the computational workload for the problem solution. Extensive computational tests of our proposed convex optimization algorithm have been carried out for dehazing of a number of hazed images in comparison with state of the art algorithms. The results have shown that our proposed algorithm outperforms the other algorithms in the image reconstruction quality and the computational efficiency.

2. THE HAZED IMAGE MODEL

Let $\mathbf{J}_c, \mathbf{I}_c \in \mathbb{R}_+^{M \times N}$ represent matrices of the haze free and hazed digital RGB color images, respectively, with nonnegative entries denoted by $J_c(m, n)$ and $I_c(m, n)$, where $c = 1, 2, 3$ is the color index, $M = 2^i$, $N = 2^j$ and $m, n \in \Omega$ are the indices in the 2-dimensional $M \times N$ pixel domain Ω . The optical model widely used to represent hazed images is:

$$\mathbf{I}_c = \mathbf{J}_c \odot \mathbf{t} + a_c(\mathbf{1} - \mathbf{t}), \quad c = 1, 2, 3, \quad (1)$$

where each a_c is the atmospheric light constant of the corresponding color channel, $\mathbf{t} \in \mathbb{R}^{M \times N}$ is the transmission distribution representing the portion of the light illumination on camera sensors, \odot denotes the elementwise multiplication operation and $\mathbf{1} \in \mathbb{R}_+^{M \times N}$ is the matrix with all 1 as entries. The objective of image dehazing is to recover the haze free image

$\mathbf{J} = \mathbf{J}_1/\mathbf{J}_2/\mathbf{J}_3$, as well as a_c and \mathbf{t} , from the observation of $\mathbf{I} = \mathbf{I}_1/\mathbf{I}_2/\mathbf{I}_3$.

The atmospheric light constant a_c is often estimated in the most haze opaque region, see [3, 9, 21]. In homogeneous atmosphere, \mathbf{t} is characterized by $\mathbf{t} = e^{-\beta \mathbf{d}}$, where $\mathbf{d} \in \mathbb{R}^{M \times N}$ is the distance map from the objectives to the camera and β is the scattering coefficient depending on the hazy medium. This implies that \mathbf{t} is elementwisely bounded by the all 0 and all 1 matrices, i.e. $\mathbf{0} \prec \mathbf{t} \preceq \mathbf{1}$. It is known that the haze is evenly distributed in atmosphere and the distance distribution \mathbf{d} is piecewise constant for most images. Thus the light transmission distribution \mathbf{t} is also piecewise constant. Considering these facts, it is assumed that the $M \times N$ dimensional distribution \mathbf{t} is 2-patch piecewise constant in the sense that $\mathbf{t}(2m+i, 2n+j) = \mathbf{t}(2m, 2n)$, for $m \in [0, M/2]$, $n \in [0, N/2]$ and $i, j = 0, 1$. Using this assumption, a simplified frequency division haze model is derived in the following.

Let \mathbf{W} be the well known discrete Haar wavelet transform (DHWT) matrix of appropriate dimension. The single level DHWT of \mathbf{I}_c and \mathbf{J}_c , $c = 1, 2, 3$, results in their transformed matrices with four $\frac{M}{2} \times \frac{N}{2}$ dimensional subband blocks, i.e.,

$$\hat{\mathbf{I}}_c = \mathbf{W}\mathbf{I}_c\mathbf{W}^T = \begin{bmatrix} \hat{\mathbf{I}}_c^a & \hat{\mathbf{I}}_c^h \\ \hat{\mathbf{I}}_c^v & \hat{\mathbf{I}}_c^d \end{bmatrix}, \quad \hat{\mathbf{J}}_c = \mathbf{W}\mathbf{J}_c\mathbf{W}^T = \begin{bmatrix} \hat{\mathbf{J}}_c^a & \hat{\mathbf{J}}_c^h \\ \hat{\mathbf{J}}_c^v & \hat{\mathbf{J}}_c^d \end{bmatrix}.$$

It can be verified that, if \mathbf{t} is 2-patch piecewise constant, its DHWT matrix has four identical subband blocks, i.e.,

$$\hat{\mathbf{t}} = \mathbf{W}\mathbf{t}\mathbf{W}^T = \begin{bmatrix} \hat{\mathbf{t}}^a & \hat{\mathbf{t}}^h \\ \hat{\mathbf{t}}^v & \hat{\mathbf{t}}^d \end{bmatrix} = \begin{bmatrix} \hat{\mathbf{t}}^a & \hat{\mathbf{t}}^a \\ \hat{\mathbf{t}}^a & \hat{\mathbf{t}}^a \end{bmatrix}, \quad \mathbf{0} \prec \hat{\mathbf{t}}^a \preceq \mathbf{1}.$$

It can be further verified that the DHWT of the haze model (1) results in

$$\begin{bmatrix} \hat{\mathbf{I}}_c^a & \hat{\mathbf{I}}_c^h \\ \hat{\mathbf{I}}_c^v & \hat{\mathbf{I}}_c^d \end{bmatrix} = \begin{bmatrix} \hat{\mathbf{J}}_c^a \odot \hat{\mathbf{t}}^a + 2a_c(\mathbf{1} - \hat{\mathbf{t}}^a) & \hat{\mathbf{J}}_c^h \odot \hat{\mathbf{t}}^a \\ \hat{\mathbf{J}}_c^v \odot \hat{\mathbf{t}}^a & \hat{\mathbf{J}}_c^d \odot \hat{\mathbf{t}}^a \end{bmatrix}. \quad (2)$$

The low frequency subband block of the above equation presents a DHWT hazed model, with the reduced dimension $\frac{M}{2} \times \frac{N}{2}$, as follows

$$\hat{\mathbf{I}}_c^a = \hat{\mathbf{J}}_c^a \odot \hat{\mathbf{t}}^a + \hat{a}_c(\mathbf{1} - \hat{\mathbf{t}}^a), \quad \hat{a}_c = 2a_c, \quad c = 1, 2, 3. \quad (3)$$

This low dimension model can enable efficient dehazing processing by recovering $\hat{\mathbf{J}}_c^a$ and $\hat{\mathbf{t}}^a$, which are sufficient for further computing the solutions for $\hat{\mathbf{t}}$, $\hat{\mathbf{J}}_c$, \mathbf{t} and \mathbf{J}_c , using the known \mathbf{I}_c , $\hat{\mathbf{I}}_c$ and the DHWT.

3. THE CONVEX OPTIMIZATION

The proposed convex optimization for dehazing is based on the simplified DHWT model (3) with the known low subband block $\hat{\mathbf{I}}_c^a$ and unknown $\hat{\mathbf{J}}_c^a$, $\hat{\mathbf{t}}^a$ and \hat{a}_c . The atmosphere light constant \hat{a}_c is first estimated following from the common procedure in [3, 9, 21]. Because of the coupling term of $\hat{\mathbf{J}}_c^d \odot \hat{\mathbf{t}}^a$ with both $\hat{\mathbf{J}}_c^d$ and $\hat{\mathbf{t}}^a$ unknown, the solution for $\hat{\mathbf{J}}_c^d$ and $\hat{\mathbf{t}}^a$ is a typical nonconvex problem.

To formulate the convex optimization problem, introduce $\hat{\mathbf{Y}}_c^a = \hat{\mathbf{I}}_c^a - \hat{a}_c \mathbf{1}$ and $\hat{\mathbf{Q}}_c^a = \hat{\mathbf{J}}_c^a \odot \hat{\mathbf{t}}^a$ and use them to write (3) into

$$\hat{\mathbf{Y}}_c^a = \hat{\mathbf{Q}}_c^a - \hat{a}_c \hat{\mathbf{t}}^a, \quad c = 1, 2, 3. \quad (4)$$

The reformulated model is linear in $\hat{\mathbf{Q}}_c^a$ and $\hat{\mathbf{t}}^a$, which enables the following convex optimization.

$$\begin{aligned} \min_{\hat{\mathbf{Q}}_c^a, \hat{\mathbf{t}}^a} \quad & \sum_{c=1,2,3} \left(\|\hat{\mathbf{Y}}_c^a - \hat{\mathbf{Q}}_c^a + \hat{a}_c \hat{\mathbf{t}}^a\|_2^2 \right) \\ & + R(\hat{\mathbf{t}}^a, \hat{\mathbf{Q}}_c^a, c = 1, 2, 3), \\ \text{s.t.} \quad & \mathbf{0} \prec \hat{\mathbf{t}}^a \preceq \mathbf{1}, \quad \mathbf{0} \preceq \hat{\mathbf{Q}}_c^a, \quad c = 1, 2, 3, \end{aligned} \quad (5)$$

where $R(\hat{\mathbf{t}}^a, \hat{\mathbf{Q}}_c^a, c = 1, 2, 3)$ denotes a convex regularization function of $\hat{\mathbf{Q}}_c^a$ and $\hat{\mathbf{t}}^a$ to be selected.

For selection of the regularization function, it is noted that the mean squared contrast of $\hat{\mathbf{J}}_c^a$ is given by [22]:

$$\begin{aligned} C_{ms} &= \sum_{c=1,2,3; m,n \in \Omega_a} (\hat{J}_c^a(m, n) - \bar{J}_c^a)^2 / N_{\Omega_a} \\ &= \sum_{c=1,2,3; m,n \in \Omega_a} \frac{(\hat{I}_c^a(m, n) - \bar{I}_c^a)^2}{(\hat{t}^a(m, n))^2 N_{\Omega_a}}, \end{aligned} \quad (6)$$

where Ω_a denotes the domain of the 2-dimensional pixel index, \bar{J}_c^a , \bar{I}_c^a are the average pixel values of $\hat{\mathbf{J}}_c^a$ and $\hat{\mathbf{I}}_c^a$, respectively, and N_{Ω_a} is the total pixel number. Since the haze effect reduces the degree of contrast in images, the image dehazing process is to enhance the level of image contrast, which is the general idea of different dehazing algorithms in the literature. It is suggested in (6) that to reduce the values of $\hat{t}^a(m, n)$ can improve the C_{ms} value of the image. It is also noted from (4) that the difference between $\hat{\mathbf{Q}}_c^a$ and $\hat{\mathbf{t}}^a$ is the constant $\hat{\mathbf{Y}}_c^a$. Thus to reduce the magnitude of $\hat{\mathbf{Q}}_c^a$ can support the reduction of $\hat{\mathbf{t}}^a$. Further, the smooth and low pass feature of $\hat{\mathbf{t}}^a$ can be promoted by regulating its total variation function. With these considerations, the regularization function $R(\hat{\mathbf{t}}^a, \hat{\mathbf{Q}}_c^a, c = 1, 2, 3)$ is specified as

$$\begin{aligned} R(\hat{\mathbf{t}}^a, \hat{\mathbf{Q}}_c^a, c = 1, 2, 3) &= \lambda_1 \|\hat{\mathbf{t}}^a\|_2^2 + \lambda_2 \|\hat{\mathbf{t}}^a\|_{TV} \\ &\quad + \lambda_3 \sum_{c=1,2,3} \|\hat{\mathbf{Q}}_c^a\|_2^2, \end{aligned}$$

where $\|\cdot\|_2$ and $\|\cdot\|_{TV}$ denote the ℓ_2 and total variation norms, respectively. It results in the following convex optimization.

$$\begin{aligned} \min_{\hat{\mathbf{Q}}_c^a, \hat{\mathbf{t}}^a} \quad & \sum_{c=1,2,3} \left(\|\hat{\mathbf{Y}}_c^a - \hat{\mathbf{Q}}_c^a + \hat{a}_c \hat{\mathbf{t}}^a\|_2^2 \right) \\ & + \lambda_1 \|\hat{\mathbf{t}}^a\|_2^2 + \lambda_2 \|\hat{\mathbf{t}}^a\|_{TV} + \lambda_3 \sum_{c=1,2,3} \|\hat{\mathbf{Q}}_c^a\|_2^2, \\ \text{s.t.} \quad & \mathbf{0} \prec \hat{\mathbf{t}}^a \preceq \mathbf{1}, \quad \mathbf{0} \preceq \hat{\mathbf{Q}}_c^a, \quad c = 1, 2, 3. \end{aligned} \quad (7)$$

The above proposed convex optimization for image dehazing is called CO-DHWT in the rest of this paper. It provides an optimal solution for $\hat{\mathbf{Q}}_c^a$, $c = 1, 2, 3$, and $\hat{\mathbf{t}}^a$. Using the obtained $\hat{\mathbf{t}}^a$ and the known $\hat{\mathbf{I}}_c$, the solution for $\hat{\mathbf{J}}_c$,

$c = 1, 2, 3$, can be computed based on (3). Its inverse DHWT results in the reconstruction of \mathbf{J}_c , $c = 1, 2, 3$.

Remark 1: The idea and derivation for the proposed CO-DHWT is directly applicable to the original hazed image model (1), which can result in the following convex optimization for image dehazing, without the DHWT but with larger image dimension.

$$\begin{aligned} \min_{\mathbf{Q}_c, \mathbf{t}} \quad & \sum_{c=1,2,3} (\|\mathbf{Y}_c - \mathbf{Q}_c + a_c \mathbf{t}\|_2^2) \\ & + \lambda_1 \|\mathbf{t}\|_2^2 + \lambda_2 \|\mathbf{t}\|_{TV} + \lambda_3 \sum_{c=1,2,3} \|\mathbf{Q}_c\|_2^2, \quad (8) \\ \text{s.t.} \quad & \mathbf{0} \prec \mathbf{t} \preceq \mathbf{1}, \quad \mathbf{0} \preceq \mathbf{Q}_c, \quad c = 1, 2, 3, \end{aligned}$$

where $\mathbf{Q}_c = \mathbf{J}_c \odot \mathbf{t}$ and $\mathbf{Y}_c = \mathbf{Q}_c - a_c \mathbf{1}$, $c = 1, 2, 3$. This convex optimization without the DHWT is called CO in the rest of this paper.

Remark 2: The idea and derivation for the proposed CO-DHWT is directly extendable to multilevel subband DHWT of the hazed image model. It can lead to transformed subband hazed image models with further reduced dimension and possible dehazing processing with further reduction of computational workload.

4. COMPUTATIONAL RESULTS

The proposed CO-DHWT (7) was implemented with the Split Bregman iteration algorithm [23] and coded with Matlab. The regularization parameters were empirically adjusted and set as $\lambda_1 = 0.02$, $\lambda_2 = 0.002$ and $\lambda_3 = 0.04$. The coded Matlab program was executed on an HP-Z420 workstation with a 3.30 GHz Intel E5-1660 CPU without using parallel processing in computations. The CO-DHWT algorithm was applied to the processing of a number of real and synthetic hazy images for performance evaluation and was compared with state of the art image dehazing algorithms, including that of Fattal in [14], He et al. in [10], Tarel and Hautiere in [21], Meng et al. in [24], Wang and Fan in [18], and Zhu et al. in [25]. Among these, the computations of the algorithms of He et al., Zhu et al. and Meng et al. used the Matlab codes provided by the authors. Performance comparisons with the other algorithms used the results presented in the corresponding publications and authors' websites.

Fig.1 (f) displays the dehazed image of the hazed "Mountain" image in Fig.1 (a) by the proposed CO-DHWT, in comparison with that of He et al., Meng et al., Fattal and Zhu et al. in Fig.1 (b) - Fig.1 (e), respectively. Fig.2 (f) displays the dehazed image of the hazed "House" image in Fig.2 (a) by the proposed CO-DHWT, in comparison with that of He et al., Meng et al., Wang and Fan. and Zhu et al. in Fig.2 (b) - (e), respectively. The results of the dehazed images in Fig. 1 and Fig. 2 can show that the proposed CO-DHWT can produce considerably better haze removal outcome than that of the other algorithms.

The proposed CO-DHWT and CO algorithms were applied to a number of hazed images of different sizes. Their average computational time durations, in second, were listed in Table 1, in comparison with that of other algorithms for the same images under the same computational conditions. It is shown that the CO-DHWT can perform much faster dehazing processing than other algorithms performed.

Table 1. Comparison of computational time (second) of different algorithms for images of different sizes

Algorithm \ Size	600×450	1024×768	1536×1024
He et al. [9]	10.04	29.46	65.4
Tarel et al. [21]	8.81	68.90	335.79
Meng et al. [24]	4.782	5.60s	10.27
Zhu et al. [25]	3.68	4.08	8.08
CO	2.25	6.85	12.9
CO-DHWT	0.70	2.08	3.72

5. CONCLUSION

By reformulating the bilinearly coupled haze free image and light transmission distribution term in the hazed image model and using an assumption on the low pass and smooth feature of the light transmission distribution, this paper has presented a convex optimization formulation for the image dehazing problem in the low pass subband of the Haar wavelet transform domain. The convex optimization enables systematic and efficient computation of the image dehazing solution and the subband wavelet transform can significantly reduce the problem dimension and the computational workload. The proposed CO-DHWT algorithm has been extensively applied to a number of hazed images, in comparison with state of the art algorithms. Its dehazing results outperform state of the art image dehazing algorithms in the better visual quality of the dehazed images and much faster processing speed.

6. ACKNOWLEDGEMENT

The authors would like to thank Dr Kaiming He, Dr Qingsong Zhu, Dr Gaofeng Meng, for providing us with their Matlab codes, and Dr Fattal and Dr Yuankai Wang for the results on their websites.

7. REFERENCES

- [1] S. Shwartz, E. Namer, and Y. Y. Schechner, "Blind haze separation," in *IEEE Computer Society Conference on Computer Vision and Pattern Recognition*, vol. 2, pp. 1984–1991, 2006.

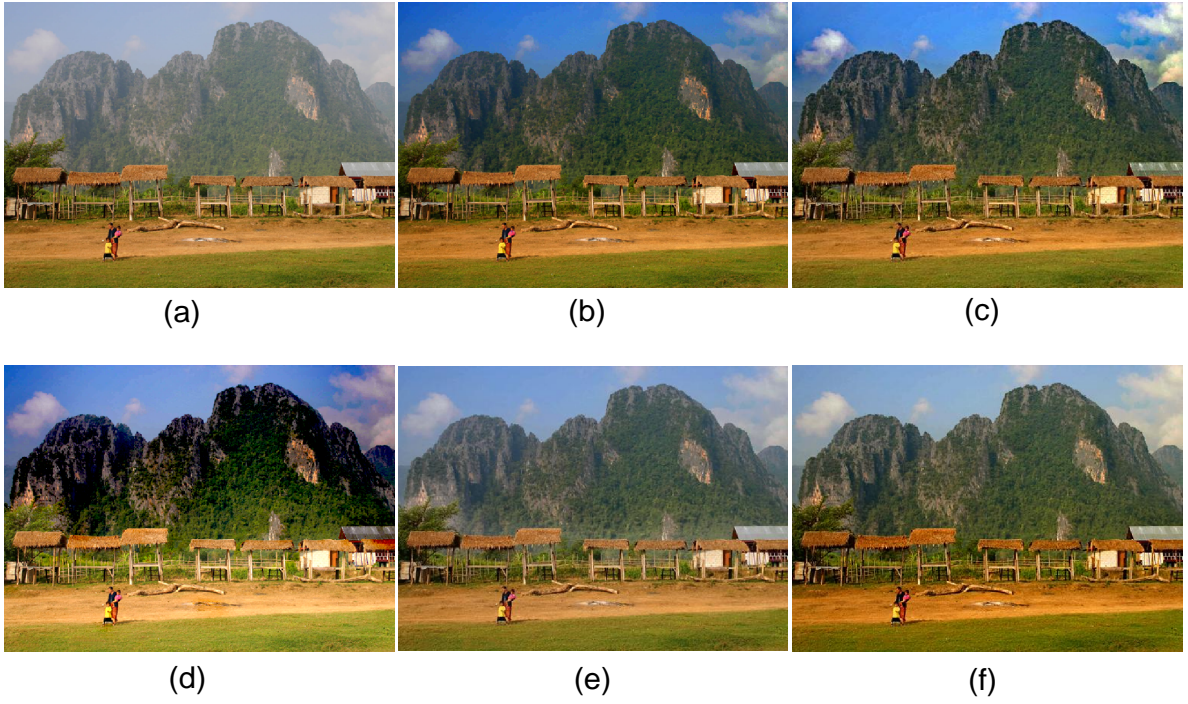


Fig. 1. Dehazing results of the "Mountain" image by different algorithms, (a) the hazed input image, (b) by He et al.'s algorithm [10], (c) by Meng et al.'s algorithm [24], (d) by Fattal's algorithm [14], (e) by Zhu et al.'s algorithm [25], (f) by CO-DHWT.



Fig. 2. Dehazing results of the "House" image by different algorithms, (a) the hazed input image, (b) by He et al.'s algorithm [10], (c) by Meng et al.'s algorithm [24], (d) by Wang and Fan's algorithm [18], (e) by Zhu et al.'s algorithm [25], (f) by CO-DHWT.

- [2] Y. Y. Schechner and Y. Averbuch, “Regularized image recovery in scattering media,” *IEEE Transactions on Pattern Analysis and Machine Intelligence*, vol. 29, pp. 1655–1660, 2007.
- [3] S. G. Narasimhan and S. K. Nayar, “Vision and the atmosphere,” *International Journal of Computer Vision*, vol. 48, pp. 233–254, 2002.
- [4] S. G. Narasimhan and S. K. Nayar, “Contrast restoration of weather degraded images,” *IEEE Transactions on Pattern Analysis and Machine Intelligence*, vol. 25, pp. 713–724, 2003.
- [5] J. Kopf, B. Neubert, B. Chen, M. Cohen, D. Cohen-Or, O. Deussen, M. Uyttendaele, and D. Lischinski, “Deep photo: Model-based photograph enhancement and viewing,” in *ACM SIGGRAPH Asia 2008 papers*, pp. 1–10, 2008.
- [6] N. Hautiere, J. P. Tarel, and D. Aubert, “Towards fog-free in-vehicle vision systems through contrast restoration,” in *IEEE Conference on Computer Vision and Pattern Recognition*, pp. 1–8, 2007.
- [7] L. Schaul, C. Fredembach, and S. Ssstrunk, “Color image dehazing using the near-infrared,” in *IEEE International Conference on Image Processing*, 2009.
- [8] F. Chen, Z. Shaojie, Z. Xiaopeng, S. Liang, and S. Susstrunk, “Near-infrared guided color image dehazing,” in *IEEE International Conference on Image Processing*, pp. 2363–2367, 2013.
- [9] K. He, J. Sun, and X. Tang, “Single image haze removal using dark channel prior,” *IEEE Transactions on Pattern Analysis and Machine Intelligence*, vol. 33, pp. 2341–2353, 2011.
- [10] K. He, J. Sun, and X. Tang, “Guided image filtering,” *IEEE Transactions on Pattern Analysis and Machine Intelligence*, vol. 35, pp. 1397 – 1409, 2012.
- [11] M. Anitharani and S. I. Padma, “Literature survey of haze removal of secure remote surveillance system,” *International Journal of Engineering Research and Technology*, vol. 2, 2013.
- [12] K. B. Gibson, D. T. Vo, and T. Q. Nguyen, “An investigation of dehazing effects on image and video coding,” *IEEE Transactions on Image Processing*, vol. 21, pp. 662–673, 2012.
- [13] J. Y. Chiang and Y. C. Chen, “Underwater image enhancement by wavelength compensation and dehazing,” *IEEE Transactions on Image Processing*, vol. 21, pp. 1756–1769, 2012.
- [14] R. Fattal, “Single image dehazing,” in *ACM Transactions on Graphics*, vol. 27, pp. 1–8, 2008.
- [15] R. T. Tan, “Visibility in bad weather from a single image,” in *IEEE Conference on Computer Vision and Pattern Recognition*, pp. 1–8, 2008.
- [16] K. Nishino, L. Kratz, and S. Lombardi, “Bayesian defogging,” *International Journal of Computer Vision*, vol. 98, pp. 263–278, 2012.
- [17] L. Caraffa and J. P. Tarel, “Markov random field model for single image defogging,” in *IEEE Intelligent Vehicle Symposium*, pp. 994–999, 2013.
- [18] Y. Wang and C. Fan, “Single image defogging by multiscale depth fusion,” *IEEE Transactions on image processing*, vol. 23, pp. 4826–4837.
- [19] F. Guo, J. Tang, and H. Peng, “A markov random field model for the restoration of foggy images,” *International Journal of Advanced Robotic Systems*, 2014.
- [20] L. Mutimbu and A. Robles-Kelly, “A relaxed factorial markov random field for colour and depth estimation from a single foggy image,” in *IEEE International Conference on Image Processing*, pp. 355–359, 2013.
- [21] J. P. Tarel and N. Hautiere, “Fast visibility restoration from a single color or gray level image,” in *IEEE International Conference on Computer Vision*, pp. 2201–2208, 2009.
- [22] J. H. Kim, W. D. Jang, J. Y. Sim, and C. S. Kim, “Optimized contrast enhancement for real-time image and video dehazing,” *Journal of Visual Communication and Image Representation*, vol. 24, pp. 410–425, 2013.
- [23] T. Goldstein and S. Osher, “The split bregman method for l1-regularized problems,” *SIAM Journal on Imaging Sciences*, vol. 2, pp. 323–343, 2009.
- [24] G. Meng, Y. Wang, J. Duan, S. Xiang, and C. Pan, “Efficient image dehazing with boundary constraint and contextual regularization,” in *IEEE International Conference on Computer Vision*, pp. 617–624, 2013.
- [25] Q. Zhu, J. Mai, and L. Shao, “A fast single image haze removal algorithm using color attenuation prior,” *IEEE Transactions on Image Processing*, vol. 24, pp. 3522–3533, 2015.